

Advanced Nanowood Materials for the Water-Energy Nexus

Xi Chen, Xiaobo Zhu, Shuaiming He, Liangbing Hu, and Zhiyong Jason Ren*

Wood materials are being reinvented to carry superior properties for a variety of new applications. Cutting-edge nanomanufacturing transforms traditional bulky and low-value woods into advanced materials that have desired structures, durability, and functions to replace nonrenewable plastics, polymers, and metals. Here, a first prospect report on how novel nanowood materials have been developed and applied in water and associated industries is provided, wherein their unique features and promises are discussed. First, the unique hierarchical structure and associated properties of the material are introduced, and then how such features can be harnessed and modified by either bottom-up or top-down manufacturing to enable different functions for water filtration, chemical adsorption and catalysis, energy and resource recovery, as well as energy-efficient desalination and environmental cleanup are discussed. The study recognizes that this is a nascent but very promising field; therefore, insights are offered to encourage more research and development. Trees harness solar energy and CO₂ and provide abundant carbon-negative materials. Once harvested and utilized, it is believed that advanced wood materials will play a vital role in enabling a circular water economy.

1. Wood as Novel and Sustainable Materials for Water Treatment and Energy and Resource Recovery

1.1. Wood Materials Carry Tremendous Potential to Complement and Replace Fossil-Based Incumbents

Access to affordable and clean water has been a grand challenge worldwide, and this problem is exacerbated every year by uneven distribution, increasing pollution, population growth, and climate change.^[1–4] The United Nations reported that nearly 6 billion people will suffer from clean water scarcity by 2050.^[5]

Dr. X. Chen, Dr. X. Zhu, Prof. Z. J. Ren

Department of Civil and Environmental Engineering and the Andlinger

Center for Energy and the Environment

Princeton University Princeton, NJ 08544, USA

E-mail: zjren@princeton.edu

Dr. S. He, Prof. L. Hu

Department of Materials Science and Engineering

University of Maryland

College Park, MD 20742, USA

The ORCID identification number(s) for the author(s) of this article can be found under https://doi.org/10.1002/adma.202001240.

DOI: 10.1002/adma.202001240

Integrated approaches are needed to address global water challenges, and material innovation has played a pivotal role in water engineering such as removing different contaminants from impaired water sources, recovering energy and chemicals from wastewater, and obtaining clean water from sea water via desalination. For example, polymer-based membranes have been widely used in water and wastewater treatment, water reuse, and desalination to remove particles, pathogens, metals, salts, and other constituents and produce clean water with desired qualities. [6-9] Plastic materials are commonly used as supporting media and reactors in filtration and biological systems for wastewater treatment and energy recovery.[10,11] Graphite carbon, ceramics, and metal materials are also broadly used in different aspects of water engineering.[12,13] While these materials are generally low-cost and durable, their performance can be limited due to intrinsic properties, and the manufacturing, usage, and disposal of these

nonrenewable materials are known to cause energy and environmental concerns.^[14,15]

In this context, natural wood and other biomass-based materials present a sustainable alternative for water and energy applications. There are estimated over 3 trillion trees on the planet, which represents over 380 trees per capita. [16] As trees grow, they absorb CO₂ from air and convert it into biomass, and recent research estimates that a worldwide planting program without impacting crop land may remove two-thirds of all the emissions from human activities that remain in the atmosphere today. [17] Plus, active research and implementation projects are underway to convert after-life wood products into bioenergy, biochar, or biomaterials, so negative emissions can be accomplished. Considering these benefits, new materials that are derived from renewable wood materials hold great promise to reduce fossil fuel and chemical use at large scale for low-carbon manufacturing.

Traditionally wood materials have been used for low-cost, low-quality fuels, tools, and construction materials, and the applications of wood are limited due to its bulkiness, heterogeneity, and low mechanical and electrical properties. However, recent advancement of nanomanufacturing greatly transformed the properties of wood and expanded its applications. Wood-based nanomaterials have been manufactured using either bottom-up assembly from nanocellulose fibers or top-down methods that functionalize existing wood hierarchical structures. A new

array of renewable materials have been developed to replace petroleum-based materials, including super wood with superb mechanical properties for advance manufacturing, [18] white wood that enables radiation cooling, [19] transparent wood for optoelectronics, [20] solar cells, [21] and windows, [22] as well as carbonized wood for energy production and storage. [23] Several excellent reviews have discussed the structures of wood-based nanomaterials and the aforementioned applications, but one emerging area of using such materials for water related applications and resource recovery has not been discussed or reviewed. This study aims to fill this gap and provide a first comprehensive review on why and how these materials carry tremendous potential for the water industry, and what opportunities and challenges are present for further research and development (Figure 1).

1.2. Nanomanufacturing Enables Versatile Structures and Functions of Wood Materials for Water-Related Applications

Wood has a natural hierarchical structure that spans several orders of magnitudes in dimensions to support different functions that a plant requires for growth. The plant cell walls are primarily composed of cellulose, hemicellulose and lignin. Cellulose forms nanometer scale microfibrils structures, which are then packed in parallel into macrofibrils to maintain the structural stability. The sizes of cellulose microfibrils are usually about 10–30 μm long and 3–10 nm wide, and they can be individually isolated to become nanocellulose fibers or crystals. $^{[24]}$ The nanocellulose materials have high aspect ratios, superb mechanical properties, and easy tunability, so there has been fast development on bottom-up assembly of these nanocellulose building blocks into functional filaments, films, membranes, as well as hydrogels and aerogels. $^{[24-26]}$

Nanocellulose materials have been increasingly used in water treatment.^[26] For example, they have been used as additives to water filtration membranes to improve permeability and reduce fouling.^[27] They can also increase membrane's tolerance on high pressure, improve adsorption capability, and enhance contaminant degradation via nanoparticle immobilization or chemical modification.^[28,29] However, the nanocellulose materials are isolated by homogenization of the wood fiber feedstock, which is a complex process and requires high energy and high chemical inputs.^[30] The following reassembly and fabrication of new materials can also be energy and chemical intensive, making the goal of sustainable manufacturing difficult.

Compared with bottom-up nanocellulose manufacturing, a new top-down approach emerged recently. By directly taking advantage of the natural hierarchical structure of the bulk wood, different materials and functions can be accomplished by encompassing the wood structures from nano- to macroscales. For example, the vertical channels (\approx 20–130 μ m) in tree trunk called vessels take charge of water and nutrients transport from ground to the tree crown (**Figure 2a**). Meanwhile, mesopores named pits (around several microns) extensively distributed on vessel walls disperse water and ions in the radial direction of the tree trunk (Figure 2d–f). As a result, these aligned channels



Xi Chen received her B.S. degrees in environmental engineering and economics from Tsinghua University. She received her Ph.D. in environmental science and engineering at Tsinghua University with Prof. Xia Huang. She joined Prof. Zhiyong Jason Ren's group as a research associate in 2016, and currently is an associate

research scholar at the Andlinger Center for Energy and the Environment, Princeton University. Her research focuses on using novel electrochemical processes and new materials for water treatment, energy generation, resource recovery, and carbon capture toward sustainable development and the water—energy nexus.



Xiaobo Zhu is a postdoctoral research associate in the Department of Civil and Environmental Engineering at Princeton University, working with Prof. Zhiyong Jason Ren. He received his B.E. from Zhejiang University of Technology in chemical engineering and his Ph.D. from the University of California, Los Angeles in civil

and environmental engineering (with Prof. David Jassby). His research interests focus on the development and application of electrically conductive membranes for water purification. He is particularly interested in electro-assisted filtration of oil/water separation and selective ion transport.



Zhiyong Jason Ren is a professor in the Department of Civil and Environmental Engineering and acting director of the Andlinger Center for Energy and the Environment at Princeton University. His research focuses on the water—energy nexus, especially in the areas of energy and resource recovery during environ-

mental processes such as wastewater treatment and reuse, water desalination, remediation, and carbon capture and utilization. He received his Ph.D. in environmental engineering from Penn State University.

and appendant pits not only endow anisotropic mechanical properties but also form the all-direction water transport pathways. The hierarchical mesoporous wood structure naturally

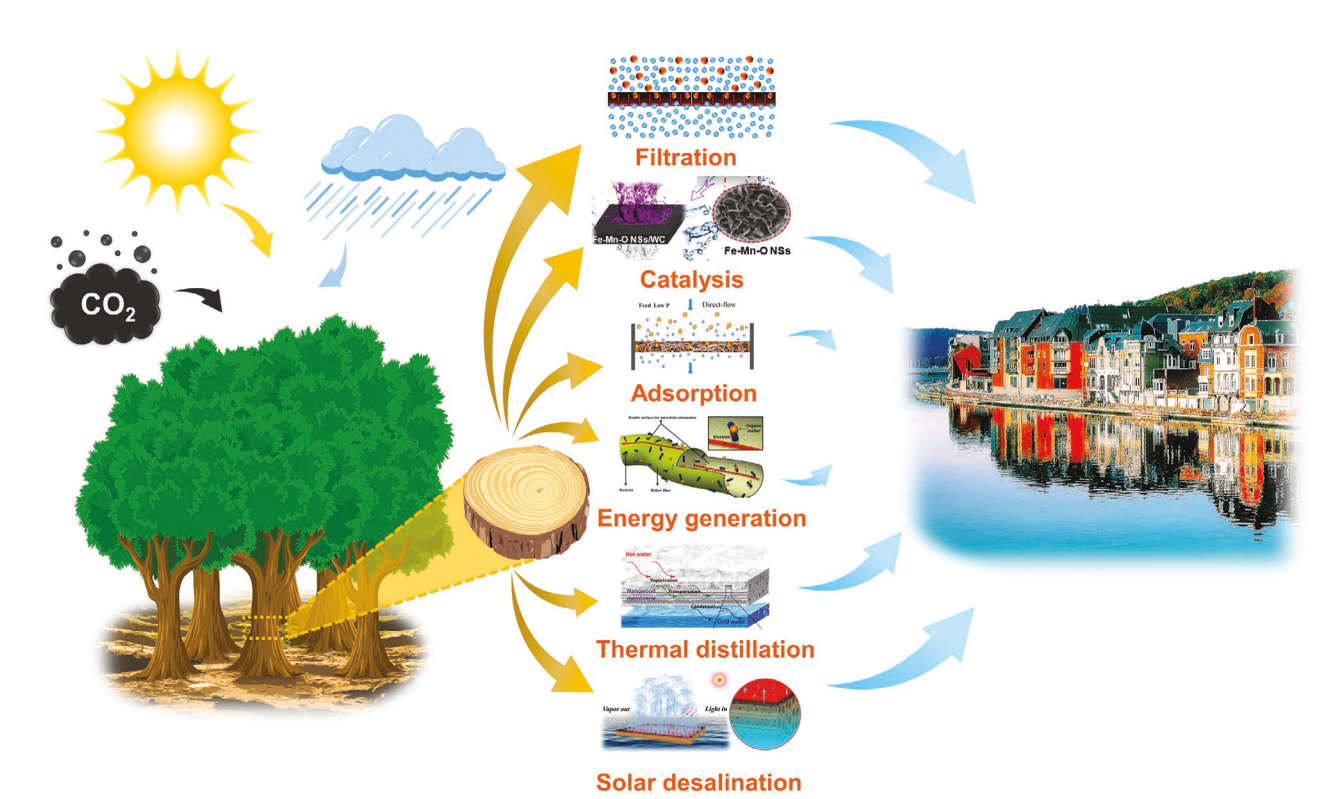


Figure 1. Schematic of the versatile properties and functions that nanowood materials can have for different water-related applications. Filtration image: Adapted with permission. [31] Copyright 2017, Royal Society of Chemistry. Catalysis image: Adapted with permission. [32] Copyright 2019, Elsevier. Adsorption image: Adapted with permission. [33] Copyright 2017, Elsevier. Energy generation image: Adapted with permission. [34] Copyright 2014, Elsevier. Thermal distillation image: Reproduced with permission. [35] Copyright 2019, The Authors, published by American Association for the Advancement of Science (AAAS) (some rights reserved; exclusive licensee American Association for the Advancement of Science. Distributed under a Creative Commons Attribution NonCommercial License 4.0 (CC BY-NC) http://creativecommons.org/licenses/by-nc/4.0/). Solar desalination image: Adapted with permission. [36] Copyright 2018, Wiley-VCH. The images on the left and right are from Pixabay.

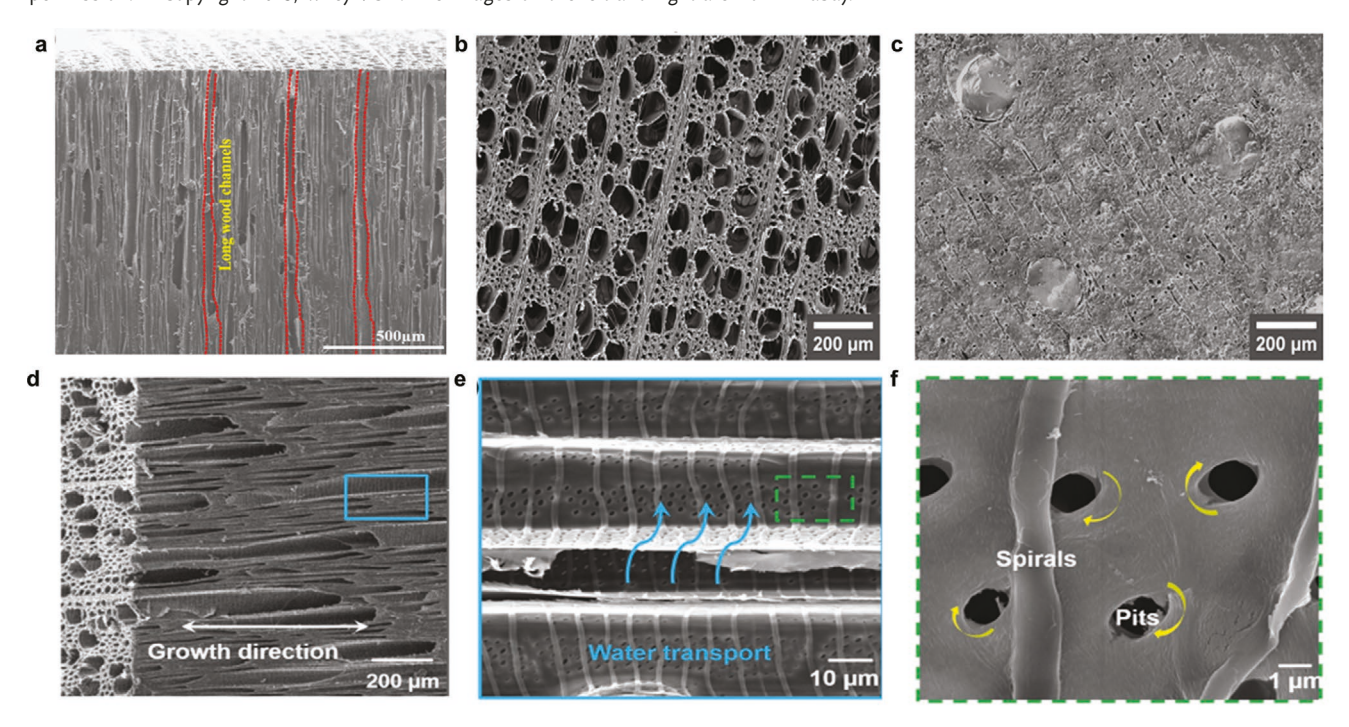


Figure 2. a) Characteristics of mesoporous wood materials: long vessel and tracheid channels along the growth direction. Reproduced with permission.^[37] Copyright 2017, American Chemical Society. b,c) Microscopic views of two wood species: b) poplar and c) cocobolo. b,c) Reproduced with permission.^[38] Copyright 2017, Cell Press. d–f) Interconnected microporous pits for water and vapor transport. d–f) Reproduced with permission.^[38] Copyright 2018, Wiley-VCH.

enables the function of particle size selection or liquid-solid separation, which are the most important functions needed in water treatment.

Trees harness the sun's energy and adsorb CO₂, and their natural wood blocks carry unique structural features. Figure 1 illustrates how wood materials can be functionalized for different water-related applications. By modifying the natural materials using engineering methods, a variety of functions can be created, including but not limited to filtration, catalysis, adsorption, energy generation, desalination, etc., these functional nanowood materials will play major roles in clean water supply, pollution control, and resource recovery to enable a carbon efficient circular water economy.

2. Engineered Nanowood for Water and Wastewater Treatment and Energy Recovery

Wood materials can be engineeringly modified to carry a variety of functions, and **Table 1** summarizes how different modification methods can tune the characteristics of wood materials for water-related applications. For example, delignification can open up wood pores for particle adsorption; carbonization can

make nanowood electrically conductive for energy generation; and chemical treatment can change the hydrophobicity and enable selective contaminant removal or water distillation. In the following sections, we discuss these modification methods, material properties, and application performance in detail. Previous reviews provided good summaries on the application of cellulose nanomaterials especially cellulose derivatives for water purification, [29] while this review focuses on the recent advancements made using new types of bulk wood nanomaterials, which demonstrated great promise on many areas related to the water—energy nexus.

2.1. Cellulose-Based Membranes for Water Filtration

As the main component of wood, cellulose nanomaterials including nanocellulose and cellulose derivative-based nanofibers are increasingly used in membrane fabrications. [24,26] Compared to other nanomaterials such as carbon nanotubes (CNTs), cellulose nanomaterials are environmentally friendly and derived from low-cost renewable sources. More ideally, cellulose-based nanomaterials carry similar features including high aspect ratios, rich hydroxyl groups, and strong mechanical strengths. [26,27,40-45]

Table 1. Summary of engineered nanowood characteristics, manufacturing processes, and water–energy related applications. Image for demonstration of polymer filling: Reproduced with permission.^[54] Copyright 2019, Royal Society of Chemistry. Image for demonstration of delignification: Reproduced with permission.^[55] Copyright 2016, Elsevier. Image for demonstration of particle immobilization: Reproduced with permission.^[37] Copyright 2017, American Chemical Society. Image for chemical treatment: Reproduced with permission.^[35] Copyright 2019, AAAS (some rights reserved; exclusive licensee American Association for the Advancement of Science. Distributed under a Creative Commons Attribution NonCommercial License 4.0 (CC BY-NC) http://creativecommons.org/licenses/by-nc/4.0/).

Natural wood		Engineered nanowood					
Characteristics	Modification	Characteristics	Application	Demonstration			
Nonconductive	Carbonization	Electro-conductive	Energy generation, storage, and delivery		[54]		
Low light adsorbing efficiency	Carbonization	Enhanced light adsorbing efficiency	Solar heating and desalination	Sunt gill	[74]		
Uneven-distributed pore size	Polymer filling	Uniform pore size	Water and salt transport		[54]		
Mesoporous and small pores	Delignification	Increased porosity and pore size	Water and vapor transport	Deling fication	[55]		
Non-catalytic	Particle immobilization	Highly reactive	Contaminant degradation	23 Michael	[37]		
Hydrophilic	Chemical treatment	Hydrophobic	Oil adsorption and vapor transport	Modern Marian	[35]		

For instance, a cellulose derivative, cellulose acetate, was first dissolved in organic solvents and cast as desalination membranes in the late 1950s and made reverse osmosis membranes viable for commercial use. [46] Nanosized cellulose materials are now used as additives in polymer matrices or coating materials. Such modifications can form highly porous structures for greater permeability, [42,43] high hydrophilicity and smoother surface to reduce membrane fouling, [27,41,43,45] as well as stronger mechanical properties to withstand higher pressures. Previous reviews summarized the early researches of cellulose-based materials in membrane filtration, [29] so in this section, we primarily focus on recent advancements of cellulose-based membranes for water filtration including ultrafiltration (UF), nanofiltration (NF), and forward osmosis (FO) membranes, as summarized in **Table 2**.

Cellulose-based membranes can be fabricated using different methods to meet function goals. These may include common vacuum filtration, blending and phase inversion, as well as spin coating and interfacial polymerization (Table 2). The base materials can be nanocellulose such as cellulose nanofibrils, nanocrystals, or cellulose derivative-based nanofibers. For example, similar to the pioneering fabrication of UF membranes using cellulose nanofibrils by Ma et al., [47] Mautner et al. constructed several UF membranes based on nanocelluloses from wood, bacterial, and other materials, and they found these then called "nanopapers" exhibited comparable transmembrane permeance with commercial tight UF membranes, and the molecular weight cut-offs ranged from 6 to 25 kDa with corresponding pore sizes of less than 10 nm. The water fluxes were 4-20 L m⁻² h⁻¹ (LMH) per MPa at a paper density of 20 grammage (Figure 3a). [48] Later studies found that mixing hydrophilic cellulose nanocrystals (CNC) into polymer matrices could optimize membrane performance in terms of water permeability, antifouling property, and mechanical strength. For instance, the introduction of hydrophilic CNC into poly(vinylidene fluoride) membranes resulted in a dramatic increase in water flux from 10 to 207 LMH.[27] Meanwhile, the membrane's irreversible fouling resistance was reduced by 48.8% when treating a model foulant bovine serum albumin (Figure 3b). However, the rejection of membrane towards BSA dropped from ≈90% to ≈40% at higher CNC loadings (Figure 3c). [27] To enhance membrane's mechanical strength and surface hydrophilicity, Bai et al. cast poly(ether sulfone) membranes with small additions of CNC from 0 to 2 wt%, and they found CNC increased hydrophilicity (Figure 3d). The resulted membranes demonstrated three times higher water flux and 1.5 times greater tensile strength at 2 wt% loading of CNC.^[49]

More delicate NF membranes could also be improved with the aid of nanocellulose materials. In short, modified membranes maintained high and stable rejections of divalent ions and small organic molecules but had much lower rejections of monovalent ions such as NaCl. By adding a CNC interlayer between the polyamide film and microporous support, Wang et al. found such an interlayer led to a much higher permeate flux of 204 LMH under 0.6 MPa with a stable salt rejection above 97% at 1000 ppm (when treating Na₂SO₄). The membrane was far outperforming the commercial NF270 and other membranes (Figure 3e). Interestingly, this membrane maintained a high separation factor of Na2SO4 over NaCl at higher salt concentrations, and the rejection of NaCl remained below 5% (Figure 3f). The smaller concentration gradient of NaCl across the membrane resulted in smaller osmotic pressure, thus this membrane could achieve much higher permeate flux.^[50] In general, commercial NF membranes offered a low to moderate NaCl rejections, which restricted the separation of NaCl and small organic molecules. To better separate small organic molecules from salt solutions, Puspasari et al. synthesized porous cellulose NF membranes using cellulose derivative-based nanofibers, trimethylsilyl cellulose. As a result, this membrane has ≈0% NaCl rejection but still can effectively reject organic molecules with a molecular weight above 300 Da.[51] This membrane could be a promising candidate for separating valuable organic compounds from the saline stream in the food and pharmaceutical industries.

Beyond pressure-driven membrane filtration processes, nanocellulose also improved the performance of FO membranes. [42] The high aspect ratio of nanocellulose materials allowed an even and high-density coating of reactive nanoparticles. When FO membranes were fabricated with Ag and Pt nanoparticle decorated nanocellulose as additives, the membranes became electrochemically reactive and antimicrobial. For desalination purposes, those membranes showed 60% higher water flux than commercial membranes. However, the membrane was found less selective for inorganic NaCl, but organic urea rejection remained above 90%. [42]

 Table 2. Summary of cellulose-based membranes for water treatment.

Process	Material	Fabrication Process	Feed solution	Rejection	Permeability	Other	Refs.
UF	Nanofibrillated cellulose	Vacuum filtration	Poly(ethylene glycol) solution	MWCO between 6 and 26 kDa	4 LMH/MPa	Pure cellulose material	[48]
UF	Hydrophilic cellulose nanocrystal	Blending-phase inversion	Bovine serum albumin (BSA) solution	40% of BSA (MWCO ≈ 68000)	21 LMH/MPa	Fouling resistance decreased by 48.8%	[27]
UF	Cellulose nanocrystal	Blending and phase inversion	DI water	_	7048 LMH/MPa	High tensile strength of 2.6 MPa	[49]
NF	Cellulose nanocrystal	Vacuum filtration and interfacial polymerization	1000 ppm Na ₂ SO ₄	97%	34 LMH/bar	Less than 5% rejection of NaCl	[50]
NF	Hydrophobic trimethylsilyl cellulose	Spin coating	1000 ppm sucrose	>80% of sucrose with MWCO of 342	1.5 LMH/bar	Nearly 0% rejection of NaCl	[51]
FO	Ag- and Pt-decorated nanocellulose	Nonsolvent induced phase separation	5% w/v NaCl draw solution	1.2–1.4 gMH (reverse salt flux)	10.24 LMH/bar	Electrochemical and antimicrobial reactive	[42]

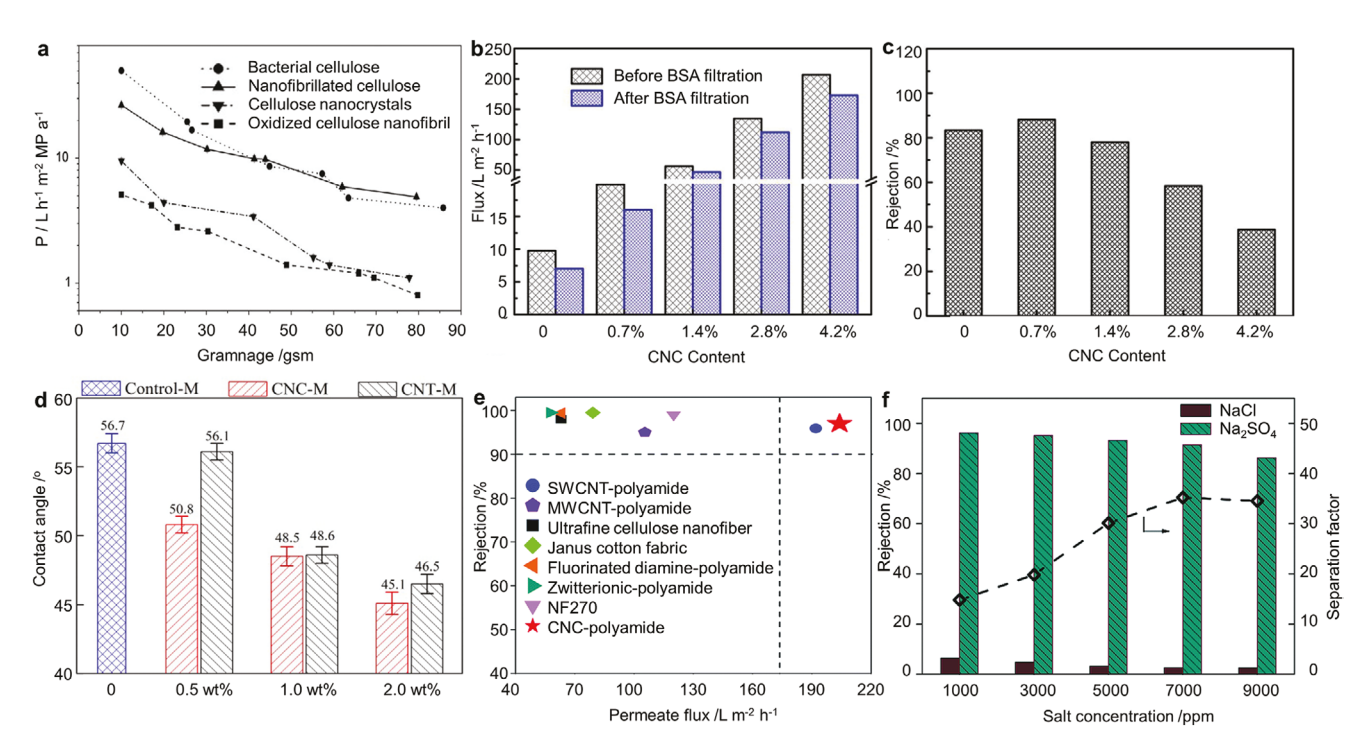


Figure 3. a) Pure water flux of cellulose membranes. Adapted with permission.^[48] Copyright 2015, Elsevier. b,c) Membrane fluxes and rejections before and after BSA filtration at different CNC loadings. b,c) Adapted from with permission.^[27] Copyright 2018, Elsevier. d) Hydrophilicity of ultrafiltration membranes with different CNC and CNT loadings. Reproduced with permission.^[49] Copyright 2016, American Chemical Society. e) Membrane performance comparison between CNC-incorporated membranes and other NF membranes, and f) its NaCl and Na₂SO₄ rejections at different salt concentrations. e,f) Adapted with permission.^[50] Copyright 2017, Royal Society of Chemistry.

2.2. Mesoporous Bulk Wood Structures for Catalytic Contaminant Removal

While cellulose-based membranes demonstrate good performance in water treatment, the manufacturing process can be energy and chemical intensive. Instead, the emerging approach of directly utilizing and modifying the bulk wood materials show good promise in several areas. The mesostructured natural wood with long and aligned channels enables high rates of water and ion transfer, and the torturous channels enhance the contact between channel surfaces and water. The high surface area with abundant hydroxyl groups in cellulose can act

as active sites for adsorption and catalyst immobilization.^[37] Hence, when decorated with catalytic nanoparticles, the distinct and highly porous structure renders the wood as a promising reactor itself for in situ contaminant degradation.^[52,53] **Table 3**summarizes existing studies that used bulk woods as base materials and decorated those using different metal catalysts as microreactors for contaminants removal. Either reduction or oxidation reaction was applied, but they both exposed advantages and challenges.

The first attempt on functionalizing bulk wood for water treatment was carried out by decorating basswood with Pd nanoparticles for methylene blue (MB) reduction (**Figure 4**a,b).^[37] By

Table 3. A brief review of adsorptive or catalytic nanowood materials and reactors for contaminant degradation.

Process	Modified material	Contaminant	Removal mechanism	Performance	Other	Refs.
Flow-through reactor	Basswood + Pd nanoparticles	30 ppm methylene blue (MB)	Chemical reduction with NaBH ₄	Up to 99.8% removal	Turnover frequency (TF) of 2.02 mol MB mol Pd ⁻¹ min ⁻¹ at a flux of 10 ⁵ LMH	[37]
Flow-through reactor	Radiate pine sapwood (softwood) + Ag nanoparticles	10 ppm MB E. coli and S. aureus	Chemical reduction with NaBH ₄	Up to 98.5% MB removal 5.2–6 orders pathogen removal	Ideal flux of 10 ⁴ LMH	[56]
Batch reactor	Carbonized basswood + Fe-Mn-O nanosheet	20 ppm tetracycline and 20 ppm MB	Chemical oxidation with H_2O_2	Up to 100% removal	97% removal of MB in stable flow-through mode	[32]
Flow-through reactor	Carbonized fir wood + TiO_2 and Mn_3O_4 nanoparticels	10 ppm MB	Chemical oxidation with H_2O_2	Up to 95% removal	TF of 0.006 mol MB mol Mn ₃ O ₄ ⁻¹ min ⁻¹ and an initial flux of 8×10^3 LMH	[57]

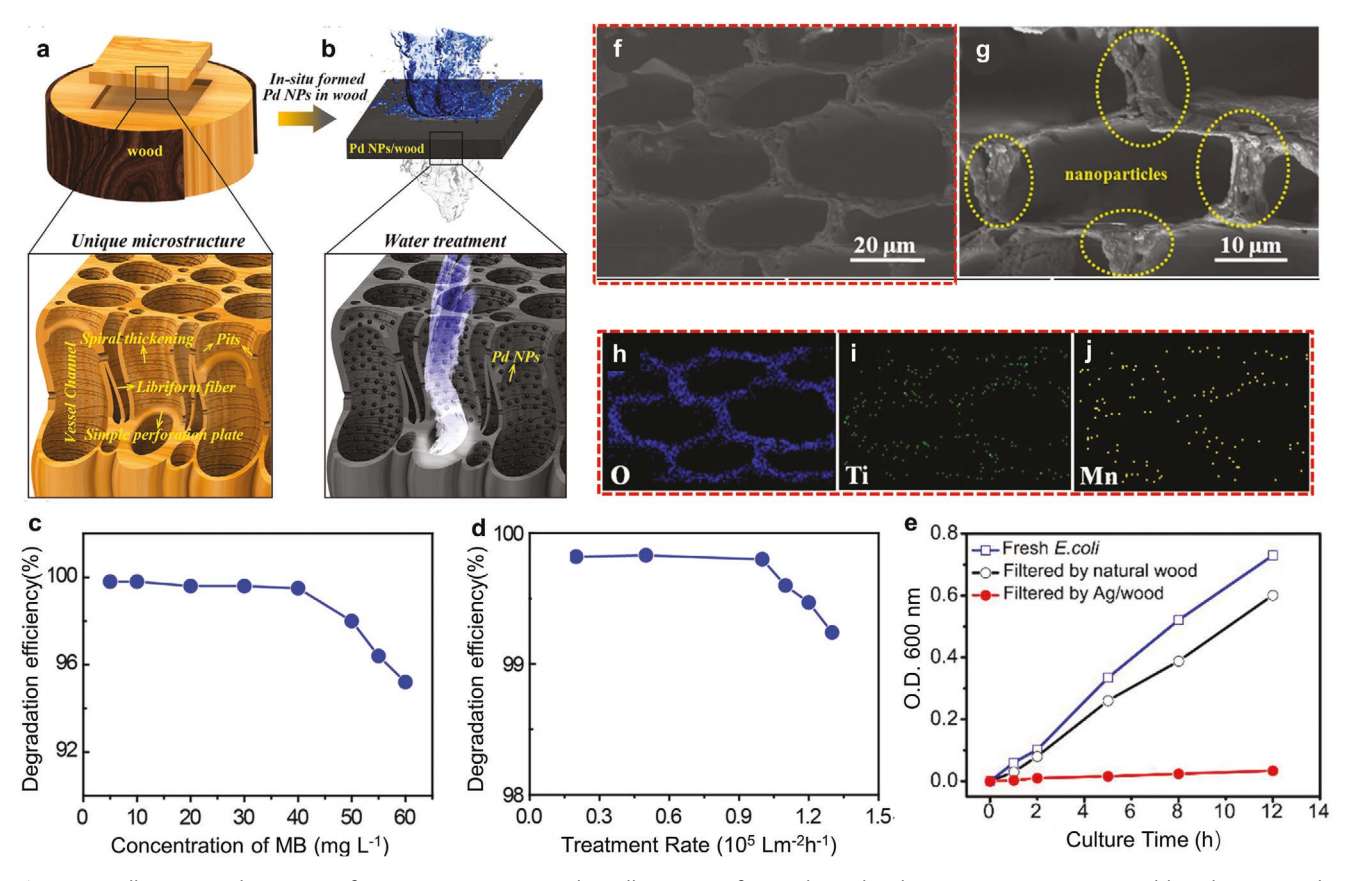


Figure 4. Bulk nanowood structures for contaminants removal. a) Illustration of natural wood with mesoporous structure and b) Pd-nanoparticle-modified wood for MB degradation via chemical reduction. c) MB degradation efficiency at different concentrations and d) permeate fluxes. a–d) Adapted with permission. [37] Copyright 2017, American Chemical Society. e) The optical density of bacteria at different culture times. a–d) Adapted with permission. [56] Copyright 2019, American Chemical Society. f,g) SEM images of wood/TiO₂/Mn₃O₄ matrix under different magnifications and h–j) the corresponding elemental mapping of O, Ti, and Mn. f–j) Reproduced with permission. [57] Copyright 2019, American Chemical Society.

immersing wood slices in PdCl2 solution and heated for 12 h at 80 °C, a uniform distribution of Pd nanoparticles (0.19 wt%) was obtained via Pd ion reduction by lignin and stable immobilization by hydroxyl groups. The modified wood was then served as a flow-through reactor for dye-containing water filtration, because Pd can activate H2 as a strong reducing agent for contaminant reduction. NaBH4 was used to react with water and actively harvest H2. The results showed that up to 99.8% of the initial 30 ppm MB was removed, and the maximum flux was 105 LMH (Figure 4c,d). The maximum conversion of reactants per catalyst concentration per time (known as, turnover frequency) was around 2 mol MB mol Pd⁻¹ min⁻¹. Similarly, radiata pine sapwood was decorated with Ag nanoparticles tested in a later study.^[56] Although the results were less desirable in MB reduction (~98.5% at an initial concentration of 10 ppm), evenly distributed Ag nanoparticles added the function of bacterial inactivation. Overall the Ag/wood filter achieved 6 and 5.2 orders of removal of Escherichia coli and Staphylococcus aureus, respectively (Figure 4e).

In addition to catalytic reduction, chemical oxidation was also tested using a different array of catalysts. In one study, fir wood was first carbonized to increase the adsorption capacity, and then $\rm Mn_3O_4/TiO_2$ nanoparticles were loaded on the walls to exhibit Fenton-like catalysis for MB removal. This reactor

was accomplished by premixing MB with H_2O_2 followed by flowing the mixture through the wood channels. Highly reactive hydroxyl radicals were generated when H_2O_2 was in contact with Mn_3O_4 , which led to a turnover frequency of 0.006 mol MB mol Pd^{-1} min⁻¹, which is quite high among Mn_3O_4 based materials but still much lower than previously mentioned reducing process (≈ 2 mol MB mol Pd^{-1} min⁻¹) (Figure 4c–g).^[57] Another study used a similar approach by making a hybrid material composed of Fe–Mn–O nanosheet and wood carbon using carbonized basswood.^[32] This Fentonlike hybrid catalyst accomplished more than 95% degradation when treating 20 ppm MB.

While catalytic reactions have been carried out in these functionalized flow-through channels in bulk wood, almost all studies used MB as a contaminant surrogate. In Table 3, NaBH₄ chemical reduction showed higher turnover frequency than $\rm H_2O_2$ oxidation, but the reduction process produced bromate as a side product. Also, a bigger problem of MB reduction is that it did not destroy the structure of MB, rather a gentle mixing of the solution in the air can result in the reformation of MB.^[58] Instead, the oxidation process could destructively break down the molecular structure of MB, with no toxic side product from hydrogen peroxide.^[59] While it is understandable that studies are still in early stages, more development and analysis are

www.advancedsciencenews.com

www.advmat.de

needed to understand the reaction mechanisms and investigate more emerging contaminants in water.

2.3. Cellulosic Composites and Functionalized Bulk Wood for Chemical Adsorption

Both cellulosic composites and bulk wood blocks offer high mechanical strength, distinct porous structures, and high surface area. These features are ideal for physical and chemical adsorptions of contaminants such as heavy metals, dyes, hydrocarbons, and dissolved organic compounds. In addition, credit to the numerous amounts of hydroxyl groups in the cellulose structure, superb adsorbing materials can be directly made from both materials via chemical functionalization. Common modification methods such as acetylation, silvlation, and polymer grafting can alter surface functional groups and provide higher adsorption capacities to target contaminants. [60] Here we briefly discuss several advanced adsorbents made from cellulosic composites, [61,62] and how similar modifications can be made on natural wood materials specifically for oil and heavy metal adsorptions. [63-65] A more detailed study focused on nanocelluose-based absorbent materials can be found elsewhere. [66]

The recent development of cellulose composites includes grafting poly(acrylic acid) (PAA) to the cellulose nanofiber mat (**Figure 5**a,b) to enhance the strength of ion exchange membranes. Those membranes exhibited a strong tensile strength of 5.19 MPa and great binding capacities to heavy metal Cd in both static and dynamic modes (\approx 25 and \approx 10 mg g⁻¹). [^{33]} Rather than changing hydroxyl groups to carboxylic groups for heavy metal adsorption, block copolymer

poly{[3-(trimethoxysilyl)propyl acrylate]-block-myrcene} was grafted onto the cellulose membrane, turning the membrane from hydrophilic into hydrophobic. As a result, these hydrophobic membranes posed excellent oil absorption capacities with a value of 6.4 g cm⁻² for crude oil. More importantly, their absorption capacities were easily recovered via immersing saturated membranes in hexane.^[67]

Bulk wood filters can also be functionalized for better adsorption. Vitas et al. chemically treated beech wood to add carboxylic acid groups on top of the hydroxyl groups with a value of up to 2.84 mmol per gram of wood. [68] These uniformly distributed carboxylic groups could take up to 95% copper ions from CuSO₄ solutions in the concentration range of 100-500 ppm and accomplished adsorption of 14 mg Cu g-1 wood. Interestingly, the 3D energy-dispersive X-ray spectroscopy revealed that the inner wood had a negligible amount of copper ions, indicating carboxylic acid groups on the inner layer of wood was inaccessible for Cu binding. More progress was made on the hydrophobic treatment of bulk wood for oil adsorption. Bulk wood was initially delignified to open up the porosity of wood blocks, and then chemicals were grafted across the wood surface to give hydrophobic and oleophilic functionality. As such, wood/epoxy biocomposite was prepared by polymerizing epoxy solution on the delignified Balsa wood template (Figure 5c). [69] The preserved natural honeycomblike structure exhibited both high Young's modulus and yield strength, which were well above other aerogel- and foambased adsorbents (Figure 5d,e). Results showed that the wood takes up 0.3 g g⁻¹ water but adsorbs oil and organic solvent in the range of 6-20 g g⁻¹ (Figure 5f).^[70] Similarly, hydrophobic wood sponges were prepared by grafting polysiloxane on the

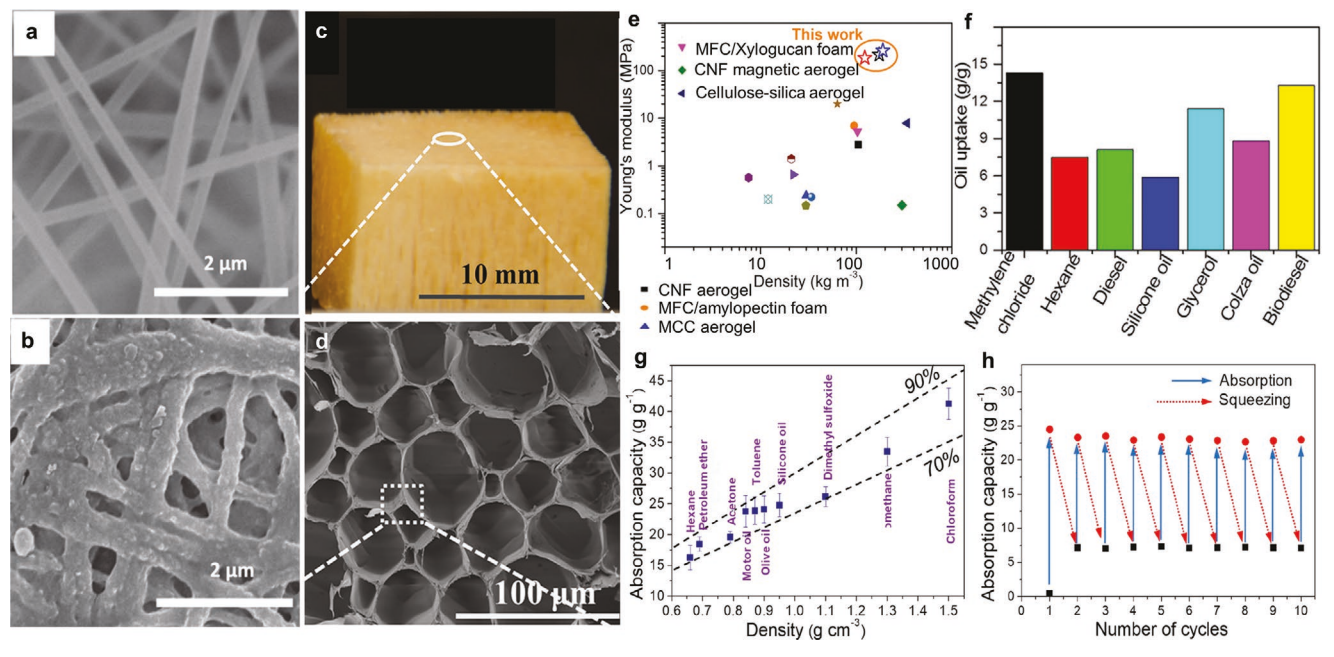


Figure 5. a,b) SEM images of cellulosic nanofiber-based membranes for heavy metal adsorption before and after modification. a,b) Reproduced with permission. [33] Copyright 2017, Elsevier. c) Wood/epoxy biocomposite, and d) its microscopic view showing honeycomb-like structure, e) the comparison of its Young's modulus among different adsorbents, and f) its oil/organic solvent adsorption capacities. c–f) Reproduced with permission. [69] Copyright 2018, American Chemical Society. g) Oil/solvent adsorption capacity of hydrophobic wood sponges, h) and the cyclic adsorption performance when treating silicon oil/water mixture. g,h) Adapted with permission. [70] Copyright 2018, American Chemical Society.

wave-like stacked wood structure using chemical vapor deposition, which demonstrated much higher oil and organic solvent adsorption capacities beyond 15 g g⁻¹ (Figure 5g). More desirably, oil or organic solvent could be easily recovered from the saturated wood by simple compression, making the wood material reusable with longevity in performance (Figure 5h). Other chemical modifications such as polydimethylsiloxane coating were also shown to be effective at creating hydrophobic function for oil–water separation.^[71]

As summarized above, bulk wood materials have been primarily studied for heavy metal and oil adsorption. However, only simple artificial chemicals have been tested, and the materials may face difficulties when actual water contaminated with multiple pollutants is tested. For example, the co-ions such as Na⁺ and K⁺ in the water may reduce the wood's binding capacity to heavy metals.^[33] Stable emulsified oil droplets that are stabilized by surfactants and salt ions in the water may reduce the separation efficiency of oil from water.^[72] Therefore, more studies are needed to test and optimize the materials in real conditions.

2.4. Carbonized Wood for Energy Generation from Wastewater Treatment

Natural wood is an electrical insulating material, but once carbonized at appropriate temperatures and conditions, monolithic carbon materials could form and become electroconductive. Attributing to the high surface area and hierarchical mesoporous structure of the wood block, the carbonized wood can become ideal materials for electrochemical applications. For example, the high conductivity, high porosity,

and low tortuosity make carbonized wood an ideal electrode material, especially for hosting electrochemical reactions that require sufficient contact areas and fast electron transfer. In energy recovery from wastewater treatment. Zhu et al. first fabricated a 3D hollow electrode for microbial fuel cells (MFCs) using kapok wood. [34] Compared with traditional graphite-based electrodes, this hollow wood fiber electrode had light weight, doubled surface area, and high conductivity (Figure 6a-c). Microscopy images showed that the unique hollow structure of the wood electrode allowed for first time dual surfaces for microbial electron transfers, which led to much higher power output (104.1 mW g⁻¹) than traditional solid fiber electrode (5.5 mW g⁻¹) on weight basis and comparable power output on surface or volume basis. Considering materials are measured in weights in engineering practice, the wood electrodes enable much higher packing density and therefore increase the overall system performance. A further study by Huang et al., demonstrated that by taking advantage of the 3D porous structure of the carbonized bulk wood, the material acted as both the electrode to support biofilm growth and electricity production, as well as a 3D microfiltration membrane to improve MFC effluent quality (Figure 6d).^[73] The porous structure with interconnected aligned channels that were retained from wood blocks enabled high water permeability and good removal performance with a pressurized flow-through operation. The results showed that more than 90% of the chemical oxygen demand (COD), total nitrogen (TN), and total phosphorus (TP) in brewery wastewater could be removed, while 248-295 mW m⁻² power was generated. More impressively, no significant fouling was observed on the membrane anode, credited to the long and well-aligned channels in the wood anode that allowed cell acclimation without blocking water flow.

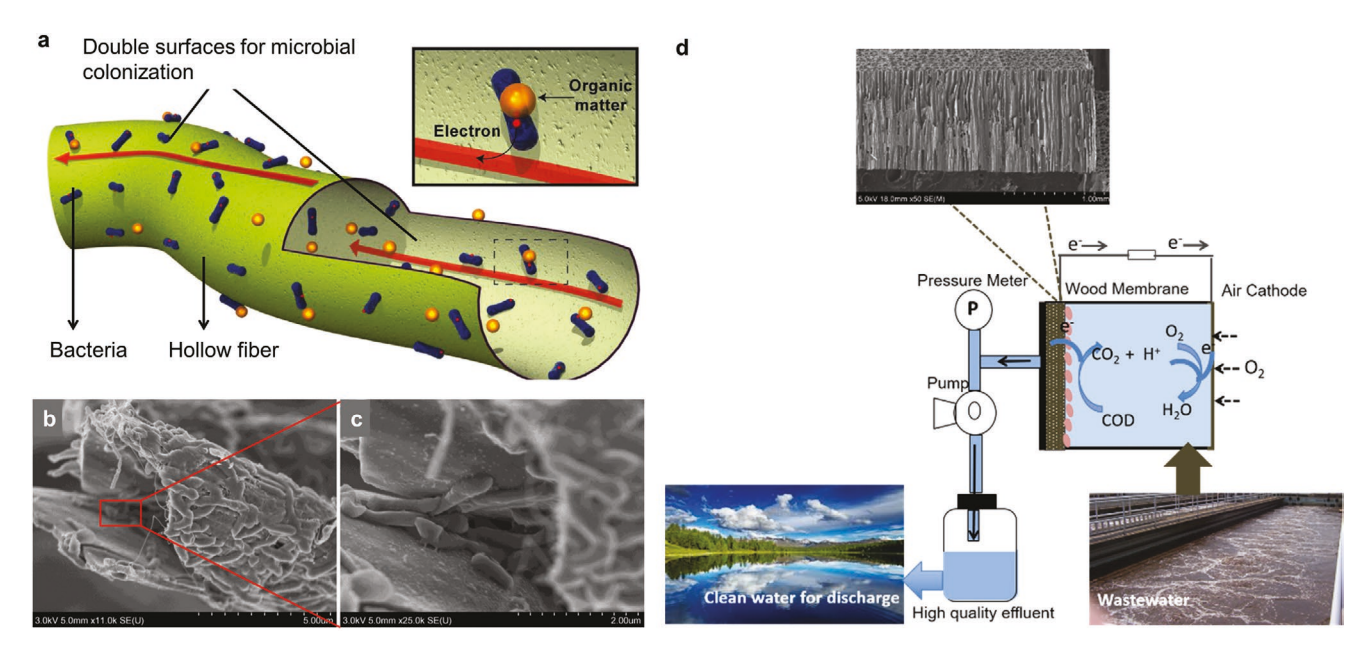


Figure 6. a) Illustration of electroactive bacteria attaching on electroconductive hollow kapok fiber electrode for current generation. b,c) SEM images of bacteria attachment on both inner and outer surface of the hollow electrode. a–c) Reproduced with permission. [34] Copyright 2014, Elsevier. d) Wood microfiltration membrane electrode that enabled both wastewater treatment and electricity production in microbial fuel cells (MFCs). Reproduced with permission. [73] Copyright 2017, Royal Society of Chemistry.

3. Nanowood for Energy-Efficient Water Desalination and Environmental Remediation

Trees play instrumental roles in the global water cycle by lifting water from underground and evaporating it to the atmosphere using sunlight as the energy source. Inspired by this capability, an emerging area of research is mimicking this solar evaporation process using functionalized bulk wood materials. [74,75] The long vessels guarantee fast water transport, while the anisotropic pore structures provide excellent thermal insulation. The renewable energy-driven desalination process carries great potential compared to existing technologies that heavily rely on fossil-fuel-based energy and materials, and when scaled it may solve water supply problems for billions of people. Moreover, similar processes can be used for resource recovery and environmental remediation, making wood evaporators even more versatile and promising.

3.1. Wood Evaporator for High Efficiency Solar-Thermal Desalination

Solar energy provides the unlimited supply of renewable energy to earth, and it has long been used in evaporation-based water purification but with low efficiency. Considering a great need of fresh water supply by billions of people, good advancement has been made in solar desalination via solar heating followed by water evaporation and collection (**Figure 7a**). Researches have focused on improving the light-to-heat conversion of photothermal materials and searching for materials with superior water transportation and thermal insulation properties. Ideal solar absorber is generally black for full spectrum (0.3–2.5 μ m)

absorption. Meanwhile, the substrate materials for the evaporator should have a lower density that allow them to float in water, so they can be exposed to solar energy. Ideally, they should also have abundant channels to facilitate fast water/vapor transportation and low thermal conductivity to limit the heat loss to the bulk water. Present efforts were dedicated to improving the desalination performance and achieved impressive progress,^[76–81] but the solar evaporators were always built upon complicated fabrication and high cost, and the scale-up of the evaporator remains a bottleneck.

The tree-inspired concept of the solar steam generator, named F-Wood/CNTs, was first reported by Hu and coworkers.^[82] By coating CNTs on the nanowood substrate, water unhinderedly transported through the hydrophilic microchannels to the black CNT layer. With CNT converting solar energy to thermal energy, water evaporation on the top layer created a capillary driving force to continuously pump saline water up for desalination. An evaporation rate of 11.22 kg m⁻² h⁻¹ was achieved under the illumination of 10 kW m⁻², and the evaporation efficiency could reach 81% (Figure 7b). The evaporation efficiencies mentioned in these studies were obtained in open systems, which tend to be higher than actual collectable water in practice. For practical solar evaporation systems, transparent covers can be used for vapor condensation and freshwater collection. But the cover and accumulated water droplet hinder solar incident, and the latent heat loss associated with vapor condensation inhibits water production.^[75]

Instead of CNTs, plasmonic metal nanoparticles like Pd, Au, Ag were further tested to decorate the 3D matrix of wood block. [83] An excellent light absorption of 99% was obtained, credit to the high efficiency by the plasmonic metals and the

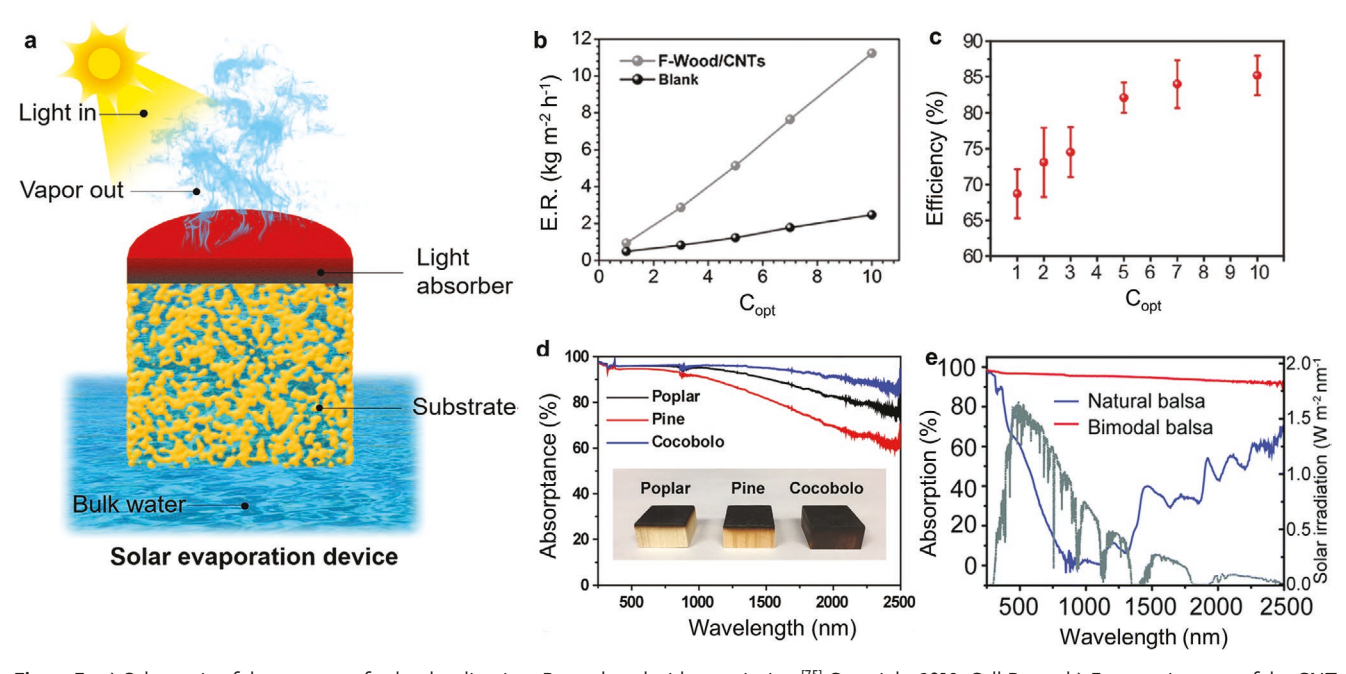


Figure 7. a) Schematic of the concept of solar desalination. Reproduced with permission. Copyright 2019, Cell Press. b) Evaporation rate of the CNT coated wood evaporator under different solar concentrations. Reproduced with permission. Copyright 2017, Wiley-VCH. c) Evaporation efficiency of plasmonic wood evaporator at different light intensities. Reproduced with permission. Copyright 2018, Wiley-VCH. d) Light absorption spectra of the wood evaporators made from different tree species. Reproduced with permission. Copyright 2017, Cell Press. e) Light absorption spectra of the carbonized wood evaporator. Reproduced with permission. Copyright 2019, Royal Society of Chemistry.

waveguide effect in the wood microchannels. In conjunction with the numerous aligned micro/nanochannels in the wood and high hydrophilicity of the material, high solar conversion efficiency of 85% under 10-sun illumination was achieved, and the system was operated for 144 h without performance declination (Figure 7c). Considering CNTs and metals are costly and nonrenewable, the researchers further modified the design by directly carbonizing the top surface of the wood into amorphous carbon and made an all-in-one wood evaporator. [39,54,84] After carbonized at 500 °C, the top surface of several wood samples from different tree species become very black and presented a total absorption (across 250-2500 nm) of 92% for poplar wood, 84% for pine wood, 96% for cocobolo wood, and 97% for balsa wood, respectively (Figure 7d-e).[39] After carbonization, the wood becomes more porous and further facilitated water transport onto the top surface of the evaporator. For all-in-one wood evaporators, the evaporation rate and efficiency improved when the wood sample had higher porosity and lower density.^[75] Therefore, balsa wood and basswood were considered better substrates for solar evaporation, largely attributed to their low densities and lower thermal conductivities.

While following the vertical lumen channels along the growth direction takes advantage of high water flux, recent findings discovered that in fact the numerous interconnected micro/nanochannels in other directions also contributed greatly to even enable higher overall solar evaporation efficiency. [39][84] Building on computational fluid dynamics (CFD) simulation findings that most of the water flux was lifted and

determined by the lumen size of the open-ended vessels in the wood evaporator (Figure 8a), Hu and co-workers investigated 13 common wood species and found that the evaporation rate improved when the wood sample had higher porosity and less density.[39] They also tested a reverse-tree design, in which the wood evaporator was placed with the growth direction laid down parallelly to the water surface. This way water was transported across vessel walls via the numerous small pores called pits (Figure 8b-d), and the layered channels in the direction perpendicular to the growth lumen direction carried much lower thermal conductivity (0.11 W m⁻¹ K⁻¹) (Figure 8e). [36] Because the microfluidic channels are perpendicular to the preferred heat transport direction, the vapor and heat pathways were decoupled from each other.[38] Surprisingly, more than twice evaporation rate was obtained this way (Figure 8f). From the CFD simulation results, the extensively distributed pits (1-2 µm in diameter) were dominant in regulating water flux, which guaranteed the rapid replenishment of water on the top surface of the wood for the fast evaporation (Figure 8h). The high thermal insulation property of the reverse-tree wood evaporator impressively confined the thermal energy at the water-vapor interface, supporting a very high evaporation rate of 1.2 kg m⁻² h⁻¹ in a short response time of 5 min and a very high evaporation efficiency of ≈80% under 1 sun incident (Figure 8g).[38] Beyond the improved performance, the scalability of the reverse-tree wood evaporator is much advantageous because it aligns with the commonly used rotate-peeling industrial cutting method for large scale wood

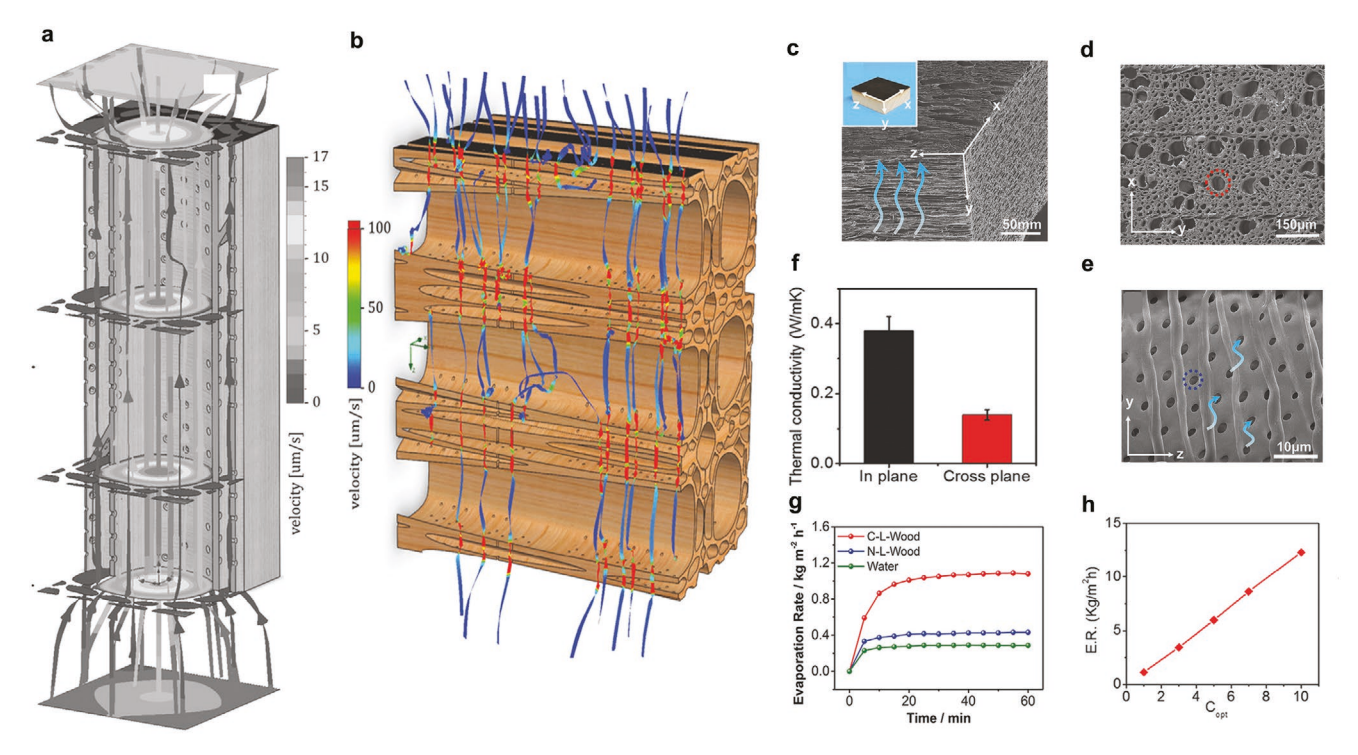


Figure 8. a) The water velocity simulation along wood channels in growth direction. b) The water velocity simulation across wood channels via pits, c–e) SEM images of the hierarchical mesoporous structure of the wood block, where abundant pits grow on the wood vessel walls (e), f) thermal conductivity of the wood in growth direction and reverse-tree direction, g) evaporation rate of the reverse-tree wood evaporator (C-L-Wood) and the conventional wood evaporator, h) stabilized evaporation rate under different sun factors. a) Reproduced with permission.^[84] Copyright 2017, Wiley-VCH. b,f,h) Reproduced with permission.^[36] Copyright 2018, Wiley-VCH.

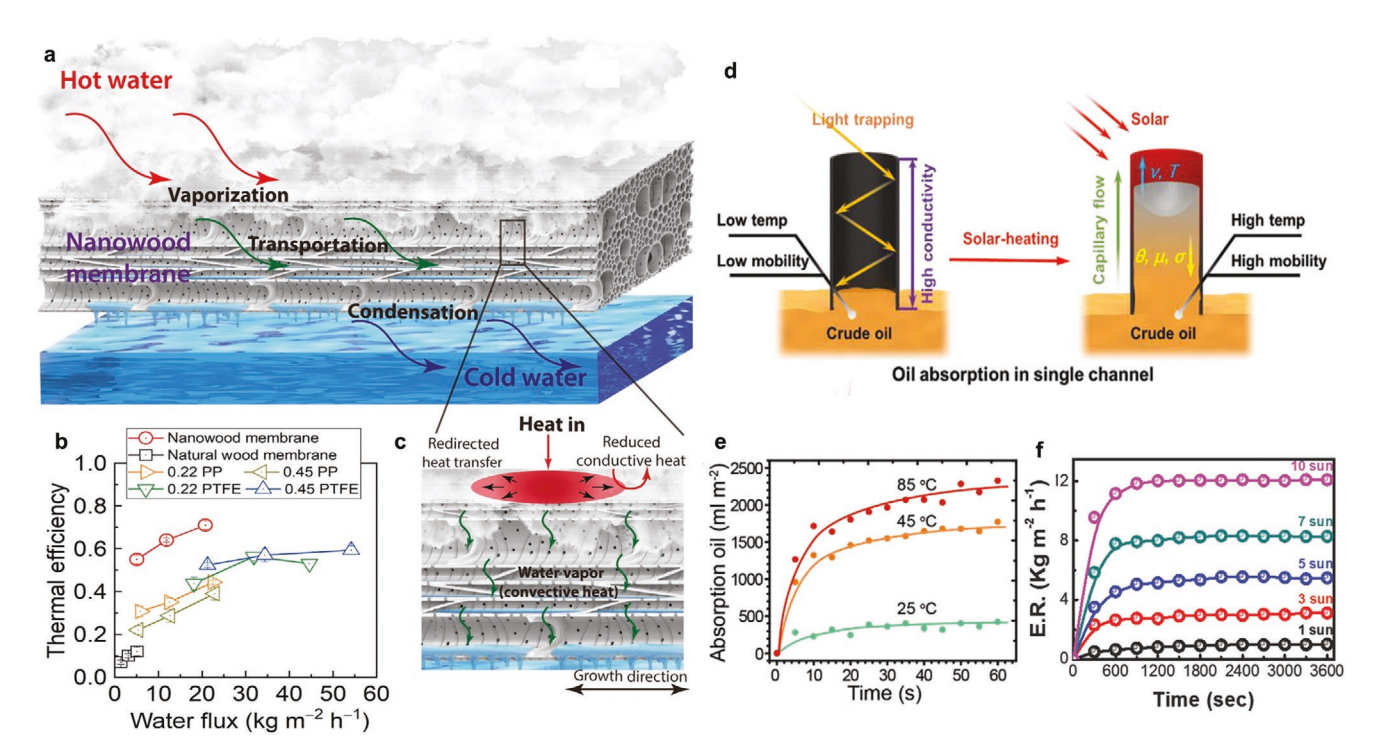


Figure 9. Advanced nanowood membrane for MD. a) Schematic of MD process, b) membrane thermal efficiency versus commercial membranes, c) illustration of heat and vapor transfer across the membrane. d) Schematic of solar-assisted crude oil absorption in the wood channels. e) Time-course oil absorption under different temperatures, and f) time-course evaporation rate of ground water lifting at various irradiation intensities. a–c) Reproduced with permission. Copyright 2019, The Authers, published by AAAS (some rights reserved; exclusive licensee American Association for the Advancement of Science. Distributed under a Creative Commons Attribution NonCommercial License 4.0 (CC BY-NC) http://creativecommons. org/licenses/by-nc/4.0/). d,e) Reproduced with permission. Copyright 2019, Wiley-VCH. f) Reproduced with permission.

board manufacturing thus can be fabricated at much larger scale and quantity.

3.2. Nanowood Membrane for Thermally Efficient Membrane Distillation

Moving beyond wood blocks, a new type of nanowood membrane was recently developed to replace polymer materials for efficient membrane distillation (MD).[85,86] MD is a water separation process that is driven by low-grade heat from solar thermal, geothermal, or waste heat sources from other operations. The temperature gradient across the membrane leads to a difference in water vapor pressure, and as the result water evaporates at the hot feed side of MD cells and diffuses through the membrane before condensing at the cold permeate side. [87] Delignified wood materials were hypothesized as a perfect candidate for new types of MD membranes, because they have highly hierarchal pore structures that allow high vapor permeability, yet the low thermal conductivity minimizes heat loss and improves efficiency. Natural American basswood was first tested along with modified nanowood that was chemically treated to remove lignin and hemicellulose. [6] The wood membrane surface was treated to become hydrophobic, so vapor could pass through but the liquid will be retained (Figure 9a,b). Results showed the nanowood membrane had high porosity (89 \pm 3%), low thermal conductivity (<0.05 W m⁻¹ K⁻¹), and high hydrophobicity. These parameters granted excellent intrinsic vapor permeability (1.44 \pm 0.09 kg m $^{-1}$ K $^{-1}$ s $^{-1}$ Pa $^{-1}$) and thermal efficiency ($\approx\!\!70\%$ at 60 °C), which were higher or comparable to commercial polymer MD membranes (Figure 9c). The membrane's vapor flux could be further improved if not hindered by the thickness ($\approx\!\!500~\mu m$ compared to $\approx\!\!100~\mu m$ of polymer membranes), and therefore advanced manufacturing that enables larger and thinner wood membrane sheets will be needed in future investigations.

3.3. Wood Evaporator for Oil Contamination Remediation

Encouraged by the fast interfacial liquid-lifting phenomenon, wood evaporators were also tested for crude oil contaminated ground water remediation. Crude oil is known to be very viscous at room temperature, so common passive absorbers faced great challenges in removing oil pollutant from contaminated water bodies. By treating the wood evaporator in growth direction to become hydrophobic and oleophilic, the temperature on the oilwater interface could be easily elevated to 45 °C under 1 sun.^[58] As a result, the crude oil was significantly thinned and flowed into the channels of the wood evaporator with an absorption rate of 1550 mL m⁻² in merely 30 s. Benefited from the low tortuosity of the wood vessels and the efficient solar-thermal conversion, this evaporator performed 10 times better than polymer-based sponge evaporators operated in similar conditions.[88] In addition, the wood evaporators were tested for ground water remediation by quickly generating clean water (vapor) from the soil. [84,89]

www.advancedsciencenews.com



www.advmat.de

The real tree stump with CNT coating as a solar absorber and the bilayer wood evaporator with carbonized surface were both tested. The superior evaporation rates of >11 kg m $^{-2}$ h $^{-1}$ and the impressive evaporation efficiencies of over 80% were achieved in these studies under 10 sun. Since ions or bacteria could hardly evaporate with the generated steam, these wood evaporators could achieve high-efficiency groundwater extraction and purification in a cost-effective and sustainable manner.^[89]

3.4. Fouling Control and Long-Term Operation

Fouling, scaling, and long-term stability have been universal concerns on filters and membranes, especially when actual impaired water sources such as seawater, groundwater, and wastewater are used. While most studies used simulated waters in the tests, there were only a handful of studies specifically addressed these issues. For most studies, the rapid water evaporation from a thin layer of brine on the top of the wood dramatically increases the local solution concentration and leads to salt precipitation.^[75] The fast salt accumulation could severely block the surface of the evaporator and thus reduces light absorption and desalination performance. To address these issues, researchers investigate the pathway of water replenishment inside the wood evaporator with the goal of developing salt-resistant or self-regenerating evaporators. Progress was made by utilizing the bimodal porous structure naturally formed in balsa wood.[54] The wider vessel channels (180-390 µm) supported fast transport of brine solution, and meanwhile the tracheid channels (18-39 µm) allowed convection/diffusion of salt and solution via the numerous pits on the channel wall. This structure was able to limit salt crystal formation for at least 7 h in continuous desalination. Another study further improved this approach by rationally drilling artificial holes (≈1 mm diameter) on the wood evaporator to form evaporation arrays. [91] This artificial bimodal wood evaporator was operated on a self-balance mechanism that bigger channels redistribute the salt concentration inside the wood substrate to minimize salt accumulation. A record 100 h continuous operation was conducted with good performance, but the solar efficiency (<80%) was not as high as other studies.

For hydrophobically treated surface, because hydrophobic membrane blocks the passage of liquid water, the performance was less affected by feed water salinity. As a result, the nanowood MD membrane showed good promise in treating highly contaminated and/or high-salinity streams, such as wastewater and seawater. However, fouling and scaling do occur as the operation goes on, and physical and chemical cleaning maybe necessary to maintain the flux. Experiments that tested fouling behavior of the nanowood membrane showed it could maintain stable flux for about 5 h before decline due to hydrophobic-hydrophobic interactions between the membrane surface and hydrophobic domains present on natural organic fouling. The organic fouling could be even exacerbated by the divalent ions such as Ca²⁺ and Mg²⁺ as they promote coagulation on the membrane surface. Fortunately, the wetted or fouled hydrophobic membranes could be restored via rinsing or backwashing using water or chemicals, followed by drying. [35] Many more studies are needed to understand the

fouling behavior and develop strategies to reduce fouling and extend system longevity.

4. Outlook

Wood materials offer abundant, versatile, and sustainable options to replace petroleum-based materials for water and associated applications. The advanced nanomanufacturing dramatically increased the value and functionalities of wood materials, and many applications have been tested in proof-ofconcept scale. While this prospective review demonstrates the great potential of these materials and applications, there is still a long way before such materials can be realistically applied in engineering systems. Further development is needed in improving material uniformity, stability, and functionality, and scalable reactor systems need to be developed to treat actual impaired water streams (saline groundwater, seawater, wastewater, etc.). The economic and environmental benefits of these new materials need to be quantified and compared with incumbent materials, and prototype systems need to be built and demonstrated.

From manufacturing point of view, the heterogeneity of wood source materials makes them unique for certain applications, but it also makes quality control a challenge. Some success has been accomplished with delignification, polymer resin filling, and source control, but more effective modification methods and testing protocols are needed to maintain the quality of the materials even though they may be derived from different raw materials. In addition, because almost all water-related applications utilize the hierarchal pore structure of the nanowood materials, fouling and scaling are inevitable issues in operation. In addition to structural and surface modification of the wood, effective cleaning and regeneration methods need to be developed to mitigate fouling and extend material lifespan.

For performance testing, to date almost all studies used artificial water and surrogate contaminants such as MB in experiments. While the data are valuable in demonstrating feasibility, the simple surrogates would not be able to represent the complexity of actual water contaminated with different chemicals. Emerging contaminants such as pharmaceuticals, personal care products, pesticides, and endocrine disrupting compounds pose major human health risks but only have low concentrations in water.^[92] Recent research on poly- and perfluoroalkyl substances,^[93] nitrosodimethylamine,^[94] and microplastics.^[95] have drawn increasing attentions. To make the nanowood materials carry specialized functions and test their feasibility in real world conditions, more testing and modifications will be desired using actual contaminated water samples and operate reactors in engineering related conditions.

With regard to applications, several key barriers will need to be overcome. First, the size of the wood materials needs to be scaled and production needs to be streamlined. While most reported studies could use centimeter scale materials, commercial membranes for water treatment can be meters long and are generally tightly packed in a treatment module. In that sense, develop membranes align with the directions in rotate-peeling tree cutting rather than cross cutting will be advantageous in

www.advancedsciencenews.com



www.advmat.de

generating long and thin wood materials. Second, long-term stability of the materials needs to be tested under various conditions. Natural wood is hydrophilic and biodegradable so is prone to swell or decay when exposed in water for a long time. Plus, nanoparticle decoration may lead to metal leaching and cause secondary contamination. Appropriate treatments like hydrophobization or densification help retain the property, but long-term stability studies are needed to understand and slow down the performance decay.

Associated with nanowood fabrication, wastewater containing salts, metals, lignin, and other constituents will be generated, and this waste stream is generally called "black liquor" in pulp and paper industry. [96] Technologies need to be developed to treat and reuse the water and recover metal, energy, and other resources to reduce impacts and improve the sustainability of the whole life cycle of nanowood materials. There is great promise in using nanowood materials to achieve effective separation and recovery of value-added products from water. For instance, salts can be recovered separately from wood evaporators, adding economic value to desalination. Further, new types of wood membrane electrodes can be fabricated to replace polymer membranes and recover gaseous products such as $\rm H_2$, $\rm NH_3$, $\rm CH_4$ for waste valorization. [97]

Nanowood materials present a transformative opportunity for material innovation in water industry and beyond, and we hope this *Progress Report* stimulates coordinated efforts in furthering the research and development of this exciting area and contributing to a circular economy.

Acknowledgements

X.C. and X. Z. contributed equally to this work. The work was supported by the US National Science Foundation under Award CEBT-1834724 and the Andlinger Center for Energy and the Environment at Princeton University.

Conflict of Interest

The authors declare no conflict of interest.

Keywords

membranes, nanocellulose, nanowood, resource recovery, water, water-energy nexus

Received: February 21, 2020 Revised: April 25, 2020 Published online:

- [1] M. M. Mekonnen, A. Y. Hoekstra, Sci. Adv. 2016, 2, e1500323.
- [2] C. J. Vörösmarty, P. Green, J. Salisbury, R. B. Lammers, *Science* 2000, 289, 284.
- [3] J. Schewe, J. Heinke, D. Gerten, I. Haddeland, N. W. Arnell, D. B. Clark, R. Dankers, S. Eisner, B. M. Fekete, F. J. Colón-González, S. N. Gosling, H. Kim, X. Liu, Y. Masaki, F. T. Portmann, Y. Satoh, T. Stacke, Q. Tang, Y. Wada, D. Wisser, T. Albrecht, K. Frieler,

- F. Piontek, L. Warszawski, P. Kabat, Proc. Natl. Acad. Sci. USA 2014, 111 3245
- [4] S. D. Richardson, S. Y. Kimura, Anal. Chem. 2016, 88, 546.
- [5] United Nations World Water Assessment Programme, The United Nations World Water Development Report 2018: Nature-Based Solutions for Water, United Nations Educational, Scientific and Cultural Organization 2018.
- [6] D. Hou, D. Jassby, R. Nerenberg, Z. J. Ren, Environ. Sci. Technol. 2019, 53, 11618.
- [7] L. F. Greenlee, D. F. Lawler, B. D. Freeman, B. Marrot, P. Moulin, Water Res. 2009, 43, 2317.
- [8] M. Elimelech, W. A. Phillip, Science 2011, 333, 712.
- [9] X. Zhu, D. Jassby, Acc. Chem. Res. 2019, 52, 1177.
- [10] M. S. Lariyah, H. A. Mohiyaden, G. Hayder, A. Hussein, H. Basri, A. F. Sabri, M. N. Noh, in *IOP Conf. Series: Earth and Environmental Science* (Eds. A. H. Shamsuddin, A. A. Rahman, H. Misran), Vol. 32, IOP, Bristol, UK 2016, p. 012005.
- [11] A. Barwal, R. Chaudhary, Rev. Environ. Sci. Bio/Technol. 2014, 13, 285.
- [12] M. Zhou, M. Chi, J. Luo, H. He, T. Jin, J. Power Sources 2011, 196, 4427.
- [13] M. M. Pendergast, E. M. V. Hoek, Energy Environ. Sci. 2011, 4, 1946.
- [14] L. Lu, J. S. Guest, C. A. Peters, X. Zhu, G. H. Rau, Z. J. Ren, Nat. Sustain. 2018, 1, 750.
- [15] W. A. Mitch, J. O. Sharp, R. R. Trussell, R. L. Valentine, L. Alvarez-Cohen, D. L. Sedlak, Environ. Eng. Sci. 2003, 20, 389.
- [16] T. W. Crowther, H. B. Glick, K. R. Covey, C. Bettigole, D. S. Maynard, S. M. Thomas, J. R. Smith, G. Hintler, M. C. Duguid, G. Amatulli, M. N. Tuanmu, W. Jetz, C. Salas, C. Stam, D. Piotto, R. Tavani, S. Green, G. Bruce, S. J. Williams, S. K. Wiser, M. O. Huber, G. M. Hengeveld, G. J. Nabuurs, E. Tikhonova, P. Borchardt, C. F. Li, L. W. Powrie, M. Fischer, A. Hemp, J. Homeier, P. Cho, A. C. Vibrans, P. M. Umunay, S. L. Piao, C. W. Rowe, M. S. Ashton, P. R. Crane, M. A. Bradford, Nature 2015, 525, 201.
- [17] P. Friedlingstein, M. Allen, J. G. Canadell, G. P. Peters, S. I. Seneviratne, *Science* 2019, 366, eaay8060.
- [18] J. Song, C. Chen, S. Zhu, M. Zhu, J. Dai, U. Ray, Y. Li, Y. Kuang, Y. Li, N. Quispe, Y. Yao, A. Gong, U. H. Leiste, H. A. Bruck, J. Y. Zhu, A. Vellore, H. Li, M. L. Minus, Z. Jia, A. Martini, T. Li, L. Hu, *Nature* 2018, 554, 224.
- [19] T. Li, Y. Zhai, S. He, W. Gan, Z. Wei, M. Heidarinejad, D. Dalgo, R. Mi, X. Zhao, J. Song, J. Dai, C. Chen, A. Aili, A. Vellore, A. Martini, R. Yang, J. Srebric, X. Yin, L. Hu, Science 2019, 364, 760.
- [20] M. Zhu, C. Jia, Y. Wang, Z. Fang, J. Dai, L. Xu, D. Huang, J. Wu, Y. Li, J. Song, Y. Yao, E. Hitz, Y. Wang, L. Hu, ACS Appl. Mater. Interfaces 2018, 10, 28566.
- [21] C. Jia, T. Li, C. Chen, J. Dai, I. M. Kierzewski, J. Song, Y. Li, C. Yang, C. Wang, L. Hu, Nano Energy 2017, 36, 366.
- [22] T. Li, M. Zhu, Z. Yang, J. Song, J. Dai, Y. Yao, W. Luo, G. Pastel, B. Yang, L. Hu, Adv. Energy Mater. 2016, 6, 1601122.
- [23] C. Chen, Y. Zhang, Y. Li, J. Dai, J. Song, Y. Yao, Y. Gong, I. Kierzewski, J. Xie, L. Hu, Energy Environ. Sci. 2017, 10, 538.
- [24] F. Jiang, T. Li, Y. Li, Y. Zhang, A. Gong, J. Dai, E. Hitz, W. Luo, L. Hu, Adv. Mater. 2018, 30, 1703453.
- [25] H. Zhu, W. Luo, P. N. Ciesielski, Z. Fang, J. Y. Zhu, G. Henriksson, M. E. Himmel, L. Hu, Chem. Rev. 2016, 116, 9305.
- [26] R. J. Moon, A. Martini, J. Nairn, J. Simonsen, J. Youngblood, Chem. Soc. Rev. 2011, 40, 3941.
- [27] J. Lv, G. Zhang, H. Zhang, C. Zhao, F. Yang, Appl. Surf. Sci. 2018, 440, 1091
- [28] H. Wei, K. Rodriguez, S. Renneckar, P. J. Vikesland, Environ. Sci.: Nano 2014, 1, 302.
- [29] A. W. Carpenter, C. F. De Lannoy, M. R. Wiesner, Environ. Sci. Technol. 2015, 49, 5277.
- [30] H. P. S. Abdul Khalil, Y. Davoudpour, M. N. Islam, A. Mustapha, K. Sudesh, R. Dungani, M. Jawaid, Carbohydr. Polym. 2014, 99, 649.

- [31] S. Mushtaq, S.-J. Yun, J. E. Yang, S.-W. Jeong, H. E. Shim, M. H. Choi, S. H. Park, Y. J. Choi, J. Jeon, *Environ. Sci.: Nano* 2017, 4, 2157.
- [32] H. Xia, Z. Zhang, J. Liu, Y. Deng, D. Zhang, P. Du, S. Zhang, X. Lu, Appl. Catal., B 2019, 259, 118058.
- [33] N. Chitpong, S. M. Husson, J. Membr. Sci. 2017, 523, 418.
- [34] H. Zhu, H. Wang, Y. Li, W. Bao, Z. Fang, C. Preston, O. Vaaland, Z. Ren, L. Hu, Nano Energy 2014, 10, 268.
- [35] D. Hou, T. Li, X. Chen, S. He, J. Dai, S. A. Mofid, D. Hou, A. Iddya, D. Jassby, R. Yang, L. Hu, Z. J. Ren, Sci. Adv. 2019, 5, eaaw3203.
- [36] H. Liu, C. Chen, G. Chen, Y. Kuang, X. Zhao, J. Song, C. Jia, X. Xu, E. Hitz, H. Xie, S. Wang, F. Jiang, T. Li, Y. Li, A. Gong, R. Yang, S. Das, L. Hu, Adv. Energy Mater. 2018, 8, 1701616.
- [37] F. Chen, A. S. Gong, M. Zhu, G. Chen, S. D. Lacey, F. Jiang, Y. Li, Y. Wang, J. Dai, Y. Yao, J. Song, B. Liu, K. Fu, S. Das, L. Hu, ACS Nano 2017, 11, 4275.
- [38] T. Li, H. Liu, X. Zhao, G. Chen, J. Dai, G. Pastel, C. Jia, C. Chen, E. Hitz, D. Siddhartha, R. Yang, L. Hu, Adv. Funct. Mater. 2018, 28, 1707134.
- [39] C. Jia, Y. Li, Z. Yang, G. Chen, Y. Yao, F. Jiang, Y. Kuang, G. Pastel, H. Xie, B. Yang, S. Das, L. Hu, Joule 2017, 1, 588.
- [40] Z. Karim, S. Claudpierre, M. Grahn, K. Oksman, A. P. Mathew, J. Membr. Sci. 2016, 514, 418.
- [41] L. Bai, Y. Liu, A. Ding, N. Ren, G. Li, H. Liang, Chemosphere 2019, 217, 76.
- [42] P. Cruz-Tato, E. O. Ortiz-Quiles, K. Vega-Figueroa, L. Santiago-Martoral, M. Flynn, L. M. Díaz-Vázquez, E. Nicolau, *Environ. Sci. Technol.* 2017, 51, 4585.
- [43] J. Lv, G. Zhang, H. Zhang, F. Yang, Carbohydr. Polym. 2017, 174, 190.
- [44] S. Mushtaq, S. J. Yun, J. E. Yang, S. W. Jeong, H. E. Shim, M. H. Choi, S. H. Park, Y. J. Choi, J. Jeon, *Environ. Sci.: Nano* 2017, 4, 2157.
- [45] Y. Jiang, Y. Zhang, B. Chen, X. Zhu, J. Membr. Sci. 2019, 588, 117222.
- [46] S. Loeb, S. Sourirajan, Adv. Chem. Ser. 1963, 15, 117.
- [47] H. Ma, C. Burger, B. S. Hsiao, B. Chu, J. Mater. Chem. 2011, 21, 7507.
- [48] A. Mautner, K. Y. Lee, T. Tammelin, A. P. Mathew, A. J. Nedoma, K. Li, A. Bismarck, React. Funct. Polym. 2015, 86, 209.
- [49] L. Bai, N. Bossa, F. Qu, J. Winglee, G. Li, K. Sun, H. Liang, M. R. Wiesner, Environ. Sci. Technol. 2017, 51, 253.
- [50] J. J. Wang, H. C. Yang, M. B. Wu, X. Zhang, Z. K. Xu, J. Mater. Chem. A 2017, 5, 16289.
- [51] T. Puspasari, N. Pradeep, K. V. Peinemann, J. Membr. Sci. 2015, 491, 132
- [52] S. He, C. Chen, G. Chen, F. Chen, J. Dai, J. Song, F. Jiang, C. Jia, H. Xie, Y. Yao, E. Hitz, G. Chen, R. Mi, M. Jiao, S. Das, L. Hu, Chem. Mater. 2020, 32, 1887.
- [53] R. Guo, X. Cai, H. Liu, Z. Yang, Y. Meng, F. Chen, Y. Li, B. Wang, Environ. Sci. Technol. 2019, 53, 2705.
- [54] S. He, C. Chen, Y. Kuang, R. Mi, Y. Liu, Y. Pei, W. Kong, W. Gan, H. Xie, E. Hitz, C. Jia, X. Chen, A. Gong, J. Liao, J. Li, Z. J. Ren, B. Yang, S. Das, L. Hu, *Energy Environ. Sci.* 2019, *12*, 1558.
- [55] M. Zhu, T. Li, C. S. Davis, Y. Yao, J. Dai, Y. Wang, F. AlQatari, J. W. Gilman, L. Hu, *Nano Energy* **2016**, *26*, 332.
- [56] W. Che, Z. Xiao, Z. Wang, J. Li, H. Wang, Y. Wang, Y. Xie, ACS Sustainable Chem. Eng. 2019, 7, 5134.
- [57] G. Liu, D. Chen, R. Liu, Z. Yu, J. Jiang, Y. Liu, J. Hu, S. Chang, ACS Sustainable Chem. Eng. 2019, 7, 6782.
- [58] P. Ncube, N. Bingwa, H. Baloyi, R. Meijboom, Appl. Catal., A 2015, 495, 63.
- [59] A. Xu, X. Li, S. Ye, G. Yin, Q. Zeng, Appl. Catal., B 2011, 102, 37.
- [60] S. Olivera, H. B. Muralidhara, K. Venkatesh, V. K. Guna, K. Gopalakrishna, K. Y. Kumar, Carbohydr. Polym. 2016, 153, 600.
- [61] F. Jiang, Y. Lo Hsieh, J. Mater. Chem. A 2014, 2, 6337.
- [62] F. Jiang, D. M. Dinh, Y. Lo Hsieh, Carbohydr. Polym. 2017, 173, 286.
- [63] X. Bai, Y. Shen, H. Tian, Y. Yang, H. Feng, J. Li, Sep. Purif. Technol. 2019. 210. 402.

- [64] W. Huang, L. Zhang, X. Lai, H. Li, X. Zeng, Chem. Eng. J. 2020, 386, 123994.
- [65] M. B. Wu, Y. M. Hong, C. Liu, J. Yang, X. P. Wang, S. Agarwal, A. Greiner, Z. K. Xu, J. Mater. Chem. A 2019, 7, 16735.
- [66] N. Mahfoudhi, S. Boufi, Cellulose 2017, 24, 1171.
- [67] R. H. Kollarigowda, S. Abraham, C. D. Montemagno, ACS Appl. Mater. Interfaces 2017, 9, 29812.
- [68] S. Vitas, T. Keplinger, N. Reichholf, R. Figi, E. Cabane, J. Hazard. Mater. 2018, 355, 119.
- [69] Q. Fu, F. Ansari, Q. Zhou, L. A. Berglund, ACS Nano 2018, 12, 2222.
- [70] H. Guan, Z. Cheng, X. Wang, ACS Nano 2018, 12, 10365.
- [71] K. Wang, X. Liu, Y. Tan, W. Zhang, S. Zhang, J. Li, Chem. Eng. J. 2019, 371, 769.
- [72] X. Zhu, A. V. Dudchenko, C. M. Khor, X. He, G. Z. Ramon, D. Jassby, Environ. Sci. Technol. 2018, 52, 11591.
- [73] Z. Huang, A. Gong, D. Hou, L. Hu, Z. J. Ren, Environ. Sci.: Water Res. Technol. 2017, 3, 940.
- [74] Z. Yu, S. Cheng, C. Li, Y. Sun, B. Li, Sol. Energy 2019, 193, 434.
- [75] C. Chen, Y. Kuang, L. Hu, Joule 2019, 3, 683.
- [76] Z. Chen, B. Dang, X. Luo, W. Li, J. Li, H. Yu, S. Liu, S. Li, ACS Appl. Mater. Interfaces 2019, 11, 26032.
- [77] P. Tao, G. Ni, C. Song, W. Shang, J. Wu, J. Zhu, G. Chen, T. Deng, Nat. Energy 2018, 3, 1031.
- [78] Q. Jiang, S. Singamaneni, Joule 2017, 1, 429.
- [79] N. Xu, X. Hu, W. Xu, X. Li, L. Zhou, S. Zhu, J. Zhu, Adv. Mater. 2017, 29, 1606762.
- [80] K. K. Liu, Q. Jiang, S. Tadepalli, R. Raliya, P. Biswas, R. R. Naik, S. Singamaneni, ACS Appl. Mater. Interfaces 2017, 9, 7675.
- [81] G. Xue, K. Liu, Q. Chen, P. Yang, J. Li, T. Ding, J. Duan, B. Qi, J. Zhou, ACS Appl. Mater. Interfaces 2017, 9, 15052.
- [82] C. Chen, Y. Li, J. Song, Z. Yang, Y. Kuang, E. Hitz, C. Jia, A. Gong, F. Jiang, J. Y. Zhu, B. Yang, J. Xie, L. Hu, Adv. Mater. 2017, 29, 1701756.
- [83] M. Zhu, Y. Li, F. Chen, X. Zhu, J. Dai, Y. Li, Z. Yang, X. Yan, J. Song, Y. Wang, E. Hitz, W. Luo, M. Lu, B. Yang, L. Hu, Adv. Energy Mater. 2018, 8, 1701028.
- [84] M. Zhu, Y. Li, G. Chen, F. Jiang, Z. Yang, X. Luo, Y. Wang, S. D. Lacey, J. Dai, C. Wang, C. Jia, J. Wan, Y. Yao, A. Gong, B. Yang, Z. Yu, S. Das, L. Hu, Adv. Mater. 2017, 29, 1704107.
- [85] A. Deshmukh, C. Boo, V. Karanikola, S. Lin, A. P. Straub, T. Tong, D. M. Warsinger, M. Elimelech, Energy Environ. Sci. 2018, 11, 1177
- [86] A. V. Dudchenko, C. Chen, A. Cardenas, J. Rolf, D. Jassby, Nat. Nanotechnol. 2017, 12, 557.
- [87] A. Alkhudhiri, N. Darwish, N. Hilal, Desalination 2012, 287, 2.
- [88] J. Chang, Y. Shi, M. Wu, R. Li, L. Shi, Y. Jin, W. Qing, C. Tang, P. Wang, J. Mater. Chem. A 2018, 6, 9192.
- [89] Y. Wang, H. Liu, C. Chen, Y. Kuang, J. Song, H. Xie, C. Jia, S. Kronthal, X. Xu, S. He, L. Hu, Adv. Sustainable Syst. 2019, 3, 1800055.
- [90] Y. Kuang, C. Chen, G. Chen, Y. Pei, G. Pastel, C. Jia, J. Song, R. Mi, B. Yang, S. Das, L. Hu, Adv. Funct. Mater. 2019, 29, 1900162.
- [91] Y. Kuang, C. Chen, S. He, E. M. Hitz, Y. Wang, W. Gan, R. Mi, L. Hu, Adv. Mater. 2019, 31, 1900498.
- [92] S. Sauvé, M. Desrosiers, Chem. Cent. J. 2014, 8, 15.
- [93] S. Huang, P. R. Jaffé, Environ. Sci. Technol. 2019, 53, 11410.
- [94] S. Almassi, Z. Li, W. Xu, C. Pu, T. Zeng, B. P. Chaplin, *Environ. Sci. Technol.* 2019, 53, 928.
- [95] V. Hidalgo-Ruz, L. Gutow, R. C. Thompson, M. Thiel, *Environ. Sci. Technol.* 2012, 46, 3060.
- [96] X. Chen, R. Katahira, Z. Ge, L. Lu, D. Hou, D. J. Peterson, M. P. Tucker, X. Chen, Z. J. Ren, *Green Chem.* 2019, 21, 1258.
- [97] D. Hou, A. Iddya, X. Chen, M. Wang, W. Zhang, Y. Ding, D. Jassby, Z. J. Ren, Environ. Sci. Technol. 2018, 52, 8930.